ENGINEERING RESEARCH INSTITUTE
UNIVERSITY OF MICHIGAN
ANN ARBOR

FINAL REPORT

WING-BODY INTERFERENCE

PART I. THEORETICAL INVESTIGATION

By

H. E. BAILEY

R. E. PHINNEY

Projects M937 and M937-1

WRIGHT AIR DEVELOPMENT CENTER, U.S. AIR FORCE
CONTRACT AF 33(038)-19747, E.O. NO. 460-31-12-11 SR-1g

January, 1954

LITHOPRINTED IN THE UNITED STATES OF AMERICA

TABLE OF CONTENTS

LIST OF FIGURES

LIST OF SYMBOLS

x,y,z	Rectangular Cartesian coordinates
x,θ,r	Cylindrical coordinates
α_B	Angle of attack of the body
α_w	Angle of attack of the wing
α_u	Angle of attack induced by the body-upwash field
Φ_1	Velocity potential of the free stream
Φ_2	Velocity potential of a doublet
Φ_3	Velocity potential of the fictitious wing
Φ_4	Interference velocity potential
V_∞	Free-stream velocity
M_∞	Free-stream Mach number
C_p	Pressure coefficient
Φ_1,Φ_2,Φ_3	Velocity potentials of the fictitious wing
f_{2n}	$2n^{th}$ Fourier coefficient of $\partial\Phi_3/\partial r\big\|_{r=1}$
I_1,I_2,I_3,I_4	Integrals defined by Equs. (18) and (19)
C_{p_2}	Pressure coefficient due to Φ_2
C_{p_3}	Pressure coefficient due to Φ_3
C_{p_4}	Pressure coefficient due to Φ_4
$C_{p_{4_{2n}}}$	$2n^{th}$ Fourier coefficient of C_{p_4}
W_{2n}	Characteristic function defined and tabulated in Reference 2.

FINAL REPORT

WING-BODY INTERFERENCE

PART I. THEORETICAL INVESTIGATION

I. INTRODUCTION

This is the first of three parts of the final report for AF Contract AF 33(038)-19747 and contains the results of the theoretical work accomplished. Part II will contain the experimental results obtained with a model composed of a cylindrical body with wings, while Part III will contain the experimental results obtained from the body simulator plate and half-wing.

The general aim of this program is to study the effect of viscosity on wing-body interference at supersonic speeds. The theoretical solution of wing-body interference problems is impossible without the aid of certain simplifying assumptions, the two most important of which are (1) an inviscid flow and (2) a linearization of the differential equations of motion. The effect which viscosity has on wing-body interference may then be found by comparing the results of experiment with the results given by a theory which neglects viscosity.

II. APPLICATION OF NIELSEN'S METHOD TO THE CASE $\alpha_B \neq 0$

1. Decomposition of Wing-Body Interference Problems

Any wing-body interference problem may be decomposed into a combination of simpler wing-body problems. This decomposition, which is presented in References 2 and 3, is illustrated diagramatically in Fig. 1. If the body is at some angle of attack α_B and the wing is at some angle of attack α_w, then

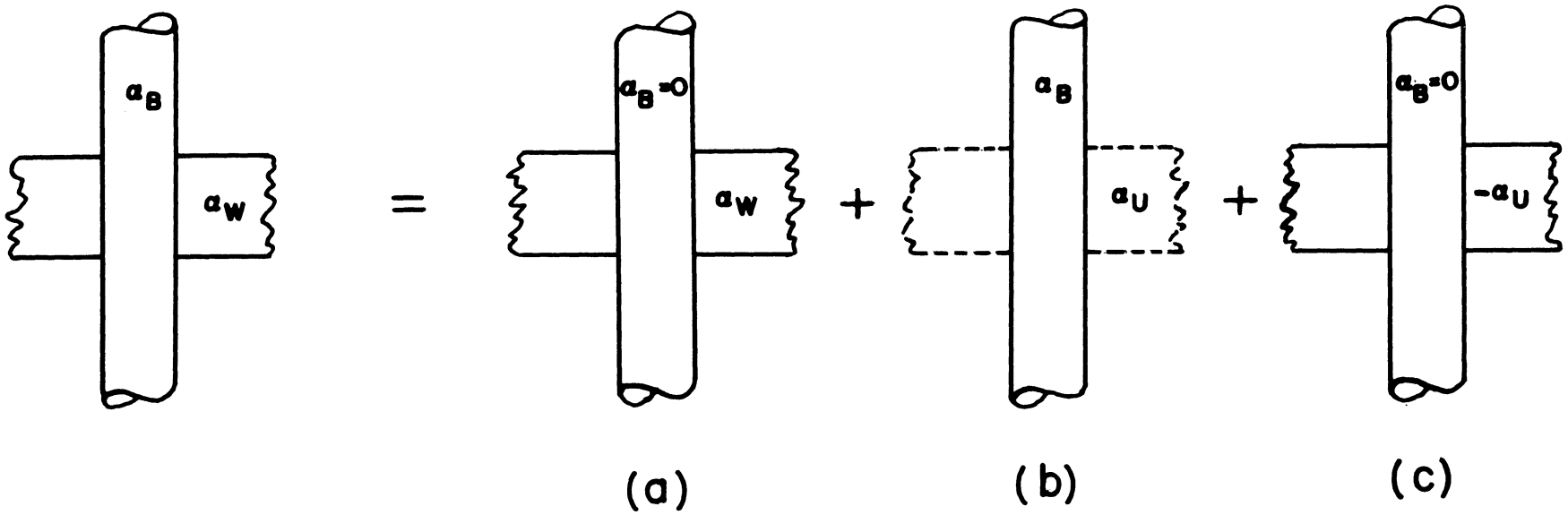

Fig. 1. Decomposition of the Wing-Body Interference Problem.

the problem may be decomposed into three separate problems: (a) body at zero angle of attack and wing at angle of attack α_w; (b) body alone at angle of attack α_B; and (c) body at zero angle of attack and wing at angle of attack $-\alpha_u$, where α_u is the angle of attack induced in the wing plane due to the body upwash field generated by the body alone at angle of attack α_B.

Problem (a) is solved by Nielsen in References 2 and 3. Solutions to problem (b) are relatively easy to obtain using the method of Reference 4. Furthermore, the method of Nielsen may be used to obtain the solution of problem (c). Since in some of the configurations tested on this project the body was at an angle of attack, it was necessary to solve problem (c).

2. Outline of Solution for Problem (c)

In order to solve problem (c) the following procedure is used: (1) the body-alone potential is found; (2) a fictitious wing potential is found which cancels the velocities induced in the wing plane by the body-alone potential; and (3) an interference potential is found which cancels the velocities induced on the cylindrical body by the wing potential but which does not induce any velocities in the wing plane. Physically the problem is that the doublet flow about an infinite circular cylinder at angle of attack α_B with respect to the free-stream direction is suddenly arrested due to the presence of a flat-plate wing with leading edge at $x = 0$.

3. Free-Stream Velocity Potential

The coordinate system used henceforth is shown in Fig. 2. The velocity potential in a uniform stream inclined at an angle α_B with respect to the x-axis is

$$\Phi_1 = V_\infty [x \cos \alpha_B + z \sin \alpha_B] = V_\infty x + V_\infty \alpha_B z . \qquad (1)$$

4. Body-Alone Velocity Potential

Now in order to make the cylinder of unit radius whose axis coincides with the x-axis a stream surface, it is necessary to add to Φ_1 the potential Φ_2 for a doublet of strength $V_\infty \alpha_B$:

$$\Phi_2 = \frac{V_\infty \alpha_B}{r} \sin \theta . \qquad (2)$$

In the linearized theory the pressure coefficient is generally taken to be a function only of the axial perturbation component. The axial component of $\Phi_1 + \Phi_2$ is

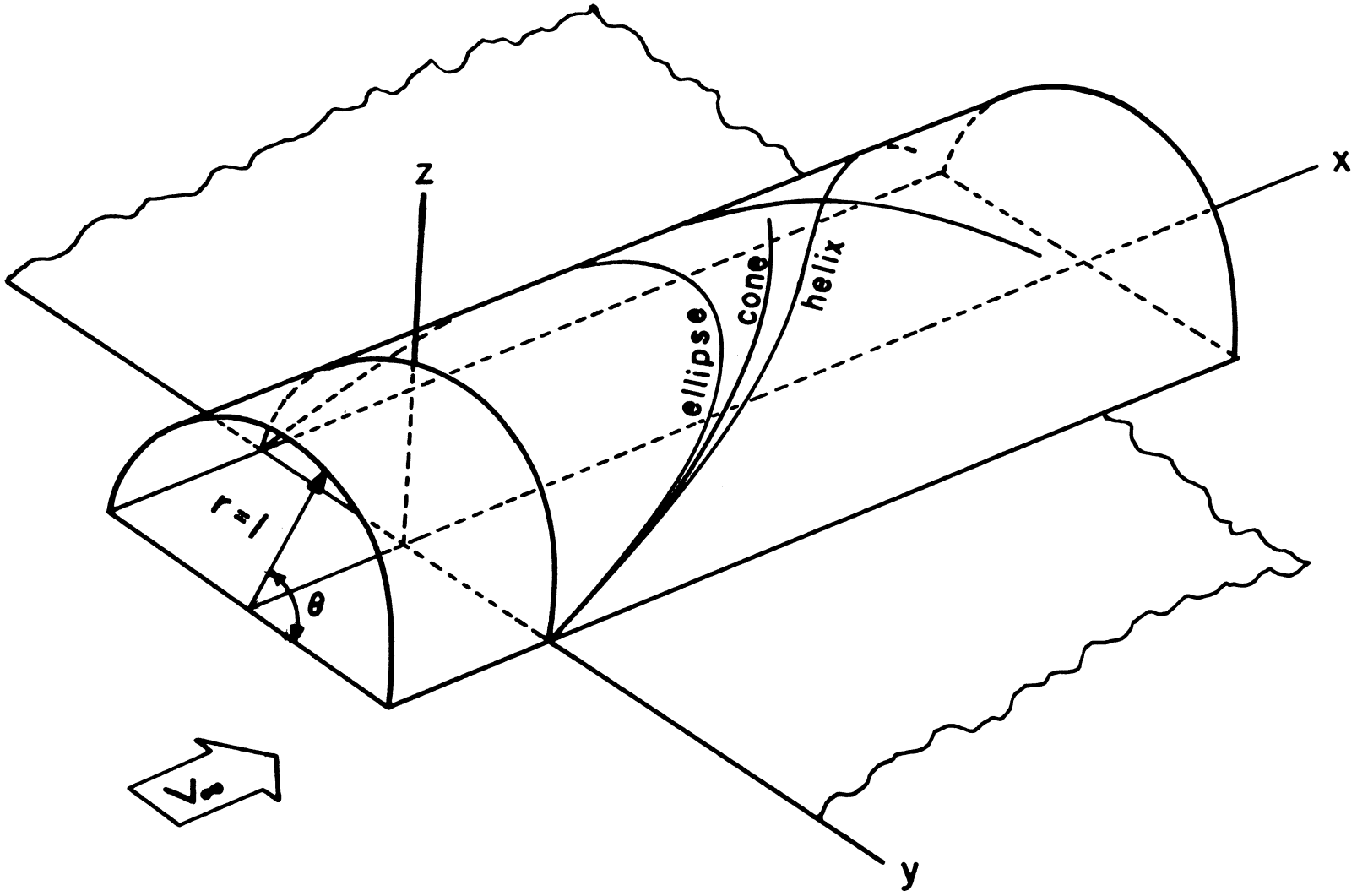

Fig. 2. Coordinate System.

$$\frac{\partial}{\partial x}\left[\Phi_1 + \Phi_2\right] = V_\infty \cos \alpha_B = V_\infty \ . \tag{3}$$

Thus, if only the axial component of the perturbation velocity is used to determine the pressure coefficient for the body alone at an angle of attack, the pressure coefficient will be zero. However, this is not in agreement with the actual pressure distribution for a body at an angle of attack, which must vary with θ. If the second and higher powers of the axial and tangential components of the perturbation velocities are included in computing the pressure coefficient, then the pressure distribution in θ for the body alone at an angle of attack will be that for a cylinder in a uniform stream of velocity $V_\infty \alpha_B$. Finding the pressure distribution in this fashion is merely an application of the local-sweepback principle.

This procedure is valid only because the body under consideration is cylindrical; i.e., the contour does not vary with x. If the body contour varied with x, it would be necessary to include first- and second-order terms according to the formula of Reference 5. Physically, this means that while the linearized form of the Bernoulli equation may be used in computing the pressure coefficient for problems (a) and (c), since in those cases the chief contribution will be from u', the linearized form of the Bernoulli equation cannot be used to compute the pressure coefficient for problem (b), since in this case the first-order perturbation terms are zero, so that the second-order terms become of paramount importance for computing the pressure coefficient on the body alone.

The component of the velocity normal to the cylinder of unit radius is readily seen to be zero, since

$$\frac{\partial}{\partial r}\left[\Phi_1 + \Phi_2\right] = V_\infty \alpha_B \sin\theta - \frac{V_\infty \alpha_B \sin\theta}{r^2} \ . \tag{4}$$

Hence,

$$\left.\frac{\partial}{\partial r}\left[\Phi_1 + \Phi_2\right]\right|_{r=1} = 0 \tag{5}$$

and the cylinder is a stream surface for the velocity potential $\Phi_1 + \Phi_2$.

5. Body-Upwash Field

The tangential velocity component on the cylinder is

$$v_\theta = \left.\frac{\partial}{\partial \theta}\left[\Phi_1 + \Phi_2\right]\right|_{r=1} = 2V_\infty \alpha_B \cos\theta \ . \tag{6}$$

It might be pointed out here that the pressure coefficient for the body alone at an angle of attack could be computed from this expression using the equation from Reference 5.

$$C_p = -\frac{2u'}{V_\infty} - \frac{v_\theta^2}{V_\infty^2} \quad . \tag{7}$$

The upwash velocity in the xy plane is given by

$$v_u = \frac{\partial}{\partial z}\left[\Phi_1 + \Phi_2\right]\Big|_{z=0} = \frac{1}{r}\frac{\partial}{\partial \theta}\left[\Phi_1 + \Phi_2\right]\Big|_{\theta=0} = V_\infty \alpha_B \left[1 + \frac{1}{y^2}\right] . \tag{8}$$

This is the value of the upwash velocity in the plane $\theta = 0$, which is inclined at an angle α_B with respect to the free-stream direction. The plane of the wing contains the free-stream velocity vector and therefore makes an angle α_B with the plane $\theta = 0$.

Now if z is perpendicular to the plane $\theta = 0$ and if z' is the direction perpendicular to the wing plane, then

$$z' = z - \alpha_B x \quad . \tag{9}$$

Hence the upwash velocity in the wing plane is

$$\frac{\partial}{\partial z'}\left[\Phi_1 + \Phi_2\right]\Big|_{z=0} = \frac{V_\infty \alpha_B}{y^2} \quad . \tag{10}$$

6. Fictitious-Wing Potential

If the wing plane is to be a stream surface, it is necessary to find the velocity potential for a wing which will just cancel the upwash velocity by inducing an equal and opposite velocity $-v_u = -(V_\infty \alpha_B)/y^2$ in the xy plane. Thus the desired potential must be that for a wing whose angle of attack varies spanwise as α_B/y^2. Since, as pointed out in Reference 2 the wing may be extended through the body in any arbitrary manner, it will be extended through the body at a constant angle of attack α_B in order to avoid infinite upwash velocities at $y = 0$.

Figure 3 is a drawing of the warped wing which will give the necessary angle-of-attack variation. It will be noticed that the wing is divided into three panels: panel I is at a constant angle of attack α_B, and panels II and III are at an angle of attack α_B / y^2.

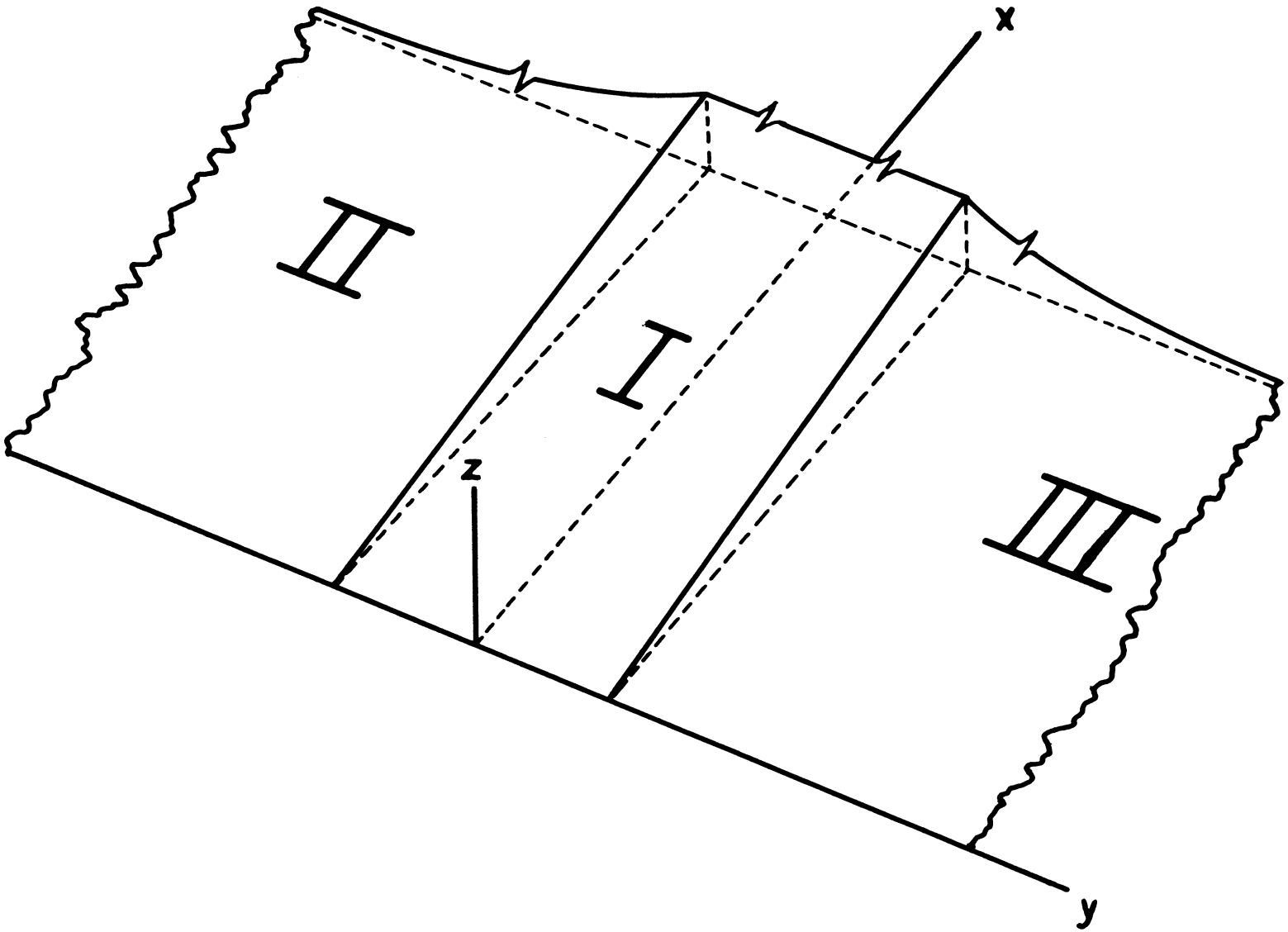

Fig. 3. Fictitious Warped Wing

The velocity potential ϕ_1 for panel I is obtained by integrating sources of constant strength $-V_\infty \alpha_B$ over the surface of panel I. If x' and y' are the coordinates of the source point, then

$$\phi_1 = \frac{V_\infty \alpha_B}{\pi} \int_{-1}^{+1} \int_{0}^{x-\sqrt{z^2+(y-y')^2}} \frac{dy'dx'}{\sqrt{(x-x')^2 - z^2 - (y-y')^2}} \; ; \quad (11)$$

$$\phi_1 = \frac{V_\infty \alpha_B}{\pi} \left\{ (y-1) \cosh^{-1} \frac{x}{\sqrt{(y-1)^2 + z^2}} - (y+1) \cosh^{-1} \right.$$

$$\cdot \frac{x}{\sqrt{(y+1)^2 + z^2}} + x \sin^{-1} \frac{y-1}{\sqrt{x^2 - z^2}} - x \sin^{-1} \frac{y+1}{\sqrt{x^2 - z^2}} \quad (12)$$

$$\left. - z \tan^{-1} \frac{x(y-1)}{z\sqrt{x^2 - z^2 - (y-1)^2}} + z \tan^{-1} \frac{x(y+1)}{z\sqrt{x^2 - z^2 - (y+1)^2}} \right\}.$$

The velocity potential for panel II is obtained by integrating sources whose strength varies as $-\alpha_B V_\infty / y^2$ over panel II; thus,

$$\phi_2 = \frac{V_\infty \alpha_B}{\pi} \int_{1}^{y+\sqrt{x^2-z^2}} \int_{0}^{x-\sqrt{z^2+(y-y')^2}} \frac{dy'dx'}{(y')^2 \sqrt{(x-x')^2 - z^2 - (y-y')^2}} \cdot \quad (13)$$

The integral is easiest to evaluate if formula 161 of Reference 6 is first used to perform the integration in x' and then, after an integration by parts together with a decomposition into partial fractions, formulae 195, 229, and 230 are used to perform the integrations in y'. The final result is

$$\phi_2 = \frac{V_\infty \alpha_B}{\pi} \left\{ \cosh^{-1} \frac{x}{\sqrt{z^2 + (y-1)^2}} + \frac{xy}{y^2 + z^2} \frac{1}{\sqrt{y^2 + z^2 - x^2}} \right.$$

$$\cos^{-1} \frac{x^2 - z^2 - y(y-1)}{\sqrt{x^2 - z^2}} - \frac{y}{y^2 + z^2} \cosh^{-1} \frac{x}{\sqrt{z^2 + (y-1)^2}} \quad (14)$$

$$\left. - \frac{\pi}{2} \frac{z}{y^2 + z^2} - \frac{z}{y^2 + z^2} \tan^{-1} \frac{x(y-1)}{z\sqrt{x^2 - z^2 - (y-1)^2}} \right\}.$$

The velocity potential for panel III may be found immediately from that for panel II simply by replacing y by -y in ϕ_2.

The total velocity potential for the entire warped wing is given by

$$\Phi_3 = \phi_1 + \phi_2 + \phi_3 = \frac{V_\infty \alpha_B}{\pi} \left\{ \left[1 - \frac{y}{y^2 + z^2} - (y - 1) \right] \right.$$

$$\cdot \cosh^{-1} \frac{x}{\sqrt{z^2 + (y - 1)^2}} + \left[1 + \frac{y}{y^2 + z^2} + (y + 1) \right]$$

$$\cdot \cosh^{-1} \frac{x}{\sqrt{z^2 + (y + 1)^2}} + \frac{xy}{y^2 + z^2} \frac{1}{\sqrt{y^2 + z^2 - x^2}}$$

$$\cdot \left[\cos^{-1} \frac{x^2 - z^2 - y(y - 1)}{\sqrt{x^2 - z^2}} - \cos^{-1} \frac{x^2 - z^2 - y(y + 1)}{\sqrt{x^2 - z^2}} \right]$$

$$-x \sin^{-1} \frac{y - 1}{\sqrt{x^2 - z^2}} + x \sin^{-1} \frac{y + 1}{\sqrt{x^2 - z^2}} - \frac{\pi z}{y^2 + z^2} + \left[z - \frac{z}{y^2 + z^2} \right]$$

$$\left. \cdot \left[\tan^{-1} \frac{x(y - 1)}{z \sqrt{x^2 - z^2 - (y - 1)^2}} + \tan^{-1} \frac{x(y + 1)}{z \sqrt{x^2 - z^2 - (y + 1)^2}} \right] \right\} . \qquad (15)$$

7. Interference Potential

If the velocity potential Φ_3 is now added to the velocity potential $\Phi_1 + \Phi_2$, the resulting flow will be parallel to the wing plane, but the addition of Φ_3 will lead to a violation of the boundary conditions on the circular cylinder. In other words, Φ_3 will induce a velocity normal to the cylinder which is given by

$$\left.\frac{\partial \Phi_3}{\partial r}\right|_{r=1} = \frac{V_\infty \alpha_B}{\pi} \left\{ \frac{x\sqrt{x^2 - 2(1 - \cos\theta)}}{1 - x^2} + \frac{x\sqrt{x^2 - 2(1 + \cos\theta)}}{1 - x^2} \right.$$

$$+ \pi \sin\theta + 2 \sin\theta \left[\tan^{-1} \frac{x(\cos\theta - 1)}{\sin\theta \sqrt{x^2 - 2(1 - \cos\theta)}} \right.$$

$$\left. \left. - \tan^{-1} \frac{x(\cos\theta + 1)}{\sin\theta \sqrt{x^2 - 2(1 + \cos 4)}} \right] + \frac{x \cos\theta \,(x^2 - 2)}{(1 - x^2)^{3/2}} \right.$$

$$\left. \cdot \left[\cos^{-1} \frac{x^2 - (1 - \cos\theta)}{\sqrt{x^2 - \sin^2\theta}} - \cos^{-1} \frac{x^2 - (1 + \cos\theta)}{\sqrt{x^2 - \sin^2\theta}} \right] . \right\} \quad (16)$$

The following discussion concerns the region in which the various terms in the above equation give a contribution to $\partial\Phi_3/\partial r\,|_{r=1}$. The first and sixth terms give a contribution only inside the Mach cone whose apex is the point x = 0, y = +1, z = 0. Furthermore, even though both of these terms appear to be unbounded at x = 1, it can be shown that together they give a finite contribution at x = 1. Similarly, the second and seventh terms give a contribution only inside the Mach cone whose apex is the point x = 0, y = -1, z = 0. The sum of these two terms gives a finite contribution at x = 1. The third term contributes to $\partial\Phi_3/\partial r\,|_{r=1}$ everywhere behind the Mach plane from the leading edge. The fourth term will give a constant contribution outside the Mach cone with apex at x = 0, y = +1, z = 0 and for the values of y in the range $-1 \leq y \leq +1$. The contribution will be variable inside this Mach cone and behind the Mach plane outside the range $-1 \leq y \leq +1$. The fifth term is similar to the fourth term except that the Mach cone in which the contribution is variable has its apex at the point x = 0, y = -1, z = 0.

8. Fourier Coefficients of $\partial\Phi_3/\partial r\,|_{r=1}$

Now, as mentioned previously, it is necessary to find an interference potential Φ_4 in order to satisfy the condition of no flow normal to the cylindrical body. This Φ_4 is exactly the potential which is given by the Nielsen method. Φ_4 will have the following properties:

(1) it will induce no velocities normal to the wing plane, and

(2) it will just cancel the velocities normal to the cylinder $r = 1$ induced by the velocity potential Φ_3.

In order to find the interference potential Φ_4 using the Nielsen method, it is necessary to obtain the Fourier expansion of $\partial\Phi_3/\partial r\,|_{r=1}$ in a cosine series of even multiples of θ; i.e.,

$$\left.\frac{\partial\Phi_3}{\partial r}\right|_{r=1} = \frac{f_0}{2} + \sum_{n=1}^{\infty} f_{2n} \cos 2n\theta \,, \tag{17}$$

where the f_{2n} are functions of x only,

$$\left.\begin{aligned} f_{2n} = {} & 4\int_0^{\sin^{-1} x} \cos 2n\theta \sin\theta\, d\theta + \frac{4}{\pi}\frac{x}{1-x^2} \\ & \cdot \int_0^{\cos^{-1}[(2-x^2)/2]} \cos 2n\theta \sqrt{x^2 - 2(1-\cos\theta)}\; d\theta \\ & + \frac{8}{\pi}\int_0^{\sin^{-1} x} \cos 2n\theta \sin\theta \tan^{-1}\frac{x(\cos\theta - 1)}{\sin\theta\sqrt{x^2 - 2(1-\cos\theta)}}\, d\theta \\ & + \frac{4}{\pi}\frac{x(x^2-2)}{(1-x^2)^{3/2}}\int_0^{\cos^{-1}[(2-x^2)/2]} \cos 2n\theta \\ & \qquad \cos\theta \cos^{-1}\frac{x^2 - (1-\cos\theta)}{\sqrt{x^2 - \sin^2\theta}}\, d\theta \end{aligned}\right\} \tag{18}$$

$$f_{2n} = I_1 + I_2 + I_3 + I_4 \,. \tag{19}$$

The integral I_1 is easily evaluated by means of formula 360 in Reference 6. The integrals I_2, I_3, and I_4 are more complicated, but may easily be shown to be expressible in terms of complete elliptic integrals of the first, second, and third kinds as long as x lies in the range $0 \le x \le 2$. For values of $x > 2$, the elliptic integrals involved in the evaluation of I_2, I_3, and I_4 become incomplete.

By means of the substitution $\cos\theta = 1 - (x^2w^2)/2$ it is readily seen that I_2 may be written in terms of complete elliptic integrals of the first and

second kinds with modulus k = x/2 and with coefficients depending only on x. Integrals I_3 and I_4 are to be integrated by parts before making use of the substitution $\cos\theta = (1 - x^2w^2)/2$. When this is done, I_3 and I_4 may be expressed in terms of complete elliptic integrals of the first, second, and third kinds with modulus k = x/2 and with coefficients depending only on x.

The first four Fourier coefficients have been computed as functions of x for intervals of x = 0.2 over the range $0 \leq x \leq 2$ with the aid of the tables in References 7 and 8. These values of the f_{2n} are plotted as functions of x in Fig. 4.

9. Computation of C_{p_4}

After the Fourier coefficients f_{2n} of $\partial\Phi_3/\partial r\,|_{r=1}$ have been found, the Fourier coefficients of the pressure coefficient $C_{p_{4_{2n}}}$ due to the interference potential Φ_4 may be obtained from

$$C_{p_{4_{2n}}}(1, \theta) = \frac{2f_{2n}(x)\cos 2n\theta}{V_\infty} - \frac{2\cos 2n\theta}{V_\infty} \cdot \int_0^x f_{2n}(\xi)\, W_{2n}(x - \xi)\, \phi\xi \,. \tag{20}$$

Equation (20) is the interference pressure coefficient as given in Reference 2. The convolution integral which appears in this equation was evaluated numerically using the values of W_{2n} tabulated in Reference 2. The integration was performed using Simpson's Rule with an interval between successive points of x = 0.2. Care must be exercised in performing this integration due to the discontinuities in the derivatives of the $f_{2n}(x)$ at x = 1.0. This difficulty was avoided by performing the integration in two parts for all values of $x > 1$. Several values of the convolution integral were checked by plotting the integrand as a function of x and integrating the resulting curve with a planimeter. The values obtained in this manner were in good agreement with those obtained using Simpson's Rule.

After the values of $C_{p_{4_{2n}}}$, which are plotted as functions of x in Fig. 5, are known, the value of C_{p_4} for any value of $0 \leq \theta \leq 90$ and $0 \leq x \leq 2$ may be obtained as the sum of the Fourier series,

$$C_{p_4} = \sum_{n=0}^{4} C_{p_{4_{2n}}} \cos 2n\theta \,. \tag{21}$$

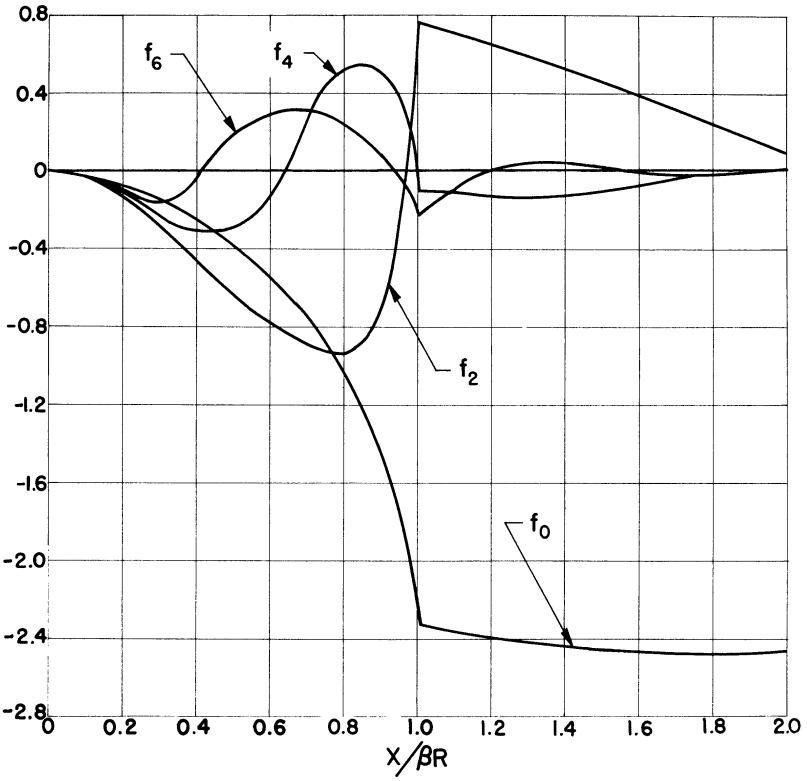

Fig. 4 – Fourier Coefficients of the Velocity Induced Normal to the Body by the Warped Wing.

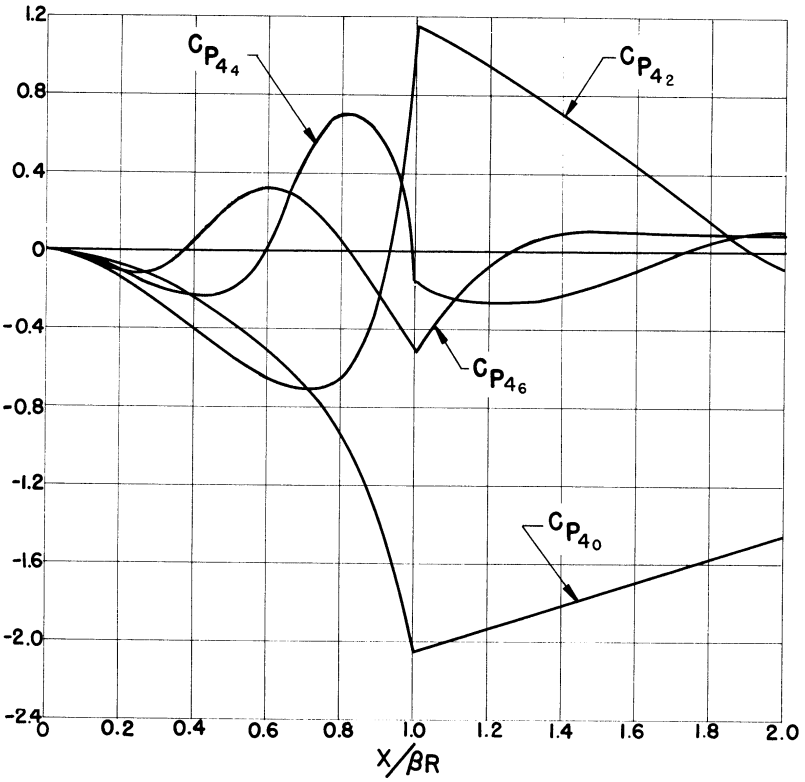

Fig. 5 – Fourier Coefficients of C_{p_4}, the Pressure Coefficient Induced on the Body by the Warped Wing.

Since only the first four terms in the Fourier series for C_{p_4} are retained, the value given by the series will not be exact. The approximation of this series to the true value of C_{p_4} will be good for large values of x, but for values of x in the range $0 \leq x \leq 1$ the approximation is not very good. The cause of this inaccurate representation of C_{p_4} for small values of x is a direct consequence of the inability of a Fourier series of only a few terms to represent accurately a function with a jump discontinuity in the immediate vicinity of the discontinuity.

10. Computation of C_p

The pressure coefficient C_{p_4} is the pressure coefficient on the body due to the interference potential Φ_4. In order to find the total pressure coefficient C_p on the body due to the presence of the wing attached to the body at an angle of attack, it is necessary to include the effect of C_{p_3}, which is the pressure coefficient induced on the body by the fictitious-wing potential Φ_3, and the effect of C_{p_2}, the pressure coefficient on the body alone at an angle of attack.

If the pressure coefficients C_{p_2}, C_{p_3}, and C_{p_4} were computed from the usual linearized formula, i.e., $C_p = 2[(\partial\Phi/\partial x)/V_\infty]$, then the total pressure coefficient would be the sum of C_{p_2}, C_{p_3}, and C_{p_4}. However, if C_{p_2} is obtained from the linearized formula, then $C_{p_2} = 0$, as pointed out in Section II, 4 above. Therefore, it is essential in computing C_{p_2} for the body alone that second-order terms in the perturbation velocities be retained.

As a result the total value of C_p has been computed as

$$\begin{aligned} C_p &= C_{p_2}, \text{ ahead of leading-edge Mach helix} \\ C_p &= C_{p_3} + C_{p_4}, \text{ behind leading-edge Mach helix.} \end{aligned} \tag{22}$$

Thus second-order terms are used in the computation of C_p ahead of the Mach helix from the juncture of the wing leading edge and the body, since in this region the first-order terms in the perturbation velocities are zero. Behind the Mach helix from the wing leading edge juncture, only first-order terms are used in the computation of C_p, since in this region the contribution of the first-order terms outweighs the contribution of the second-order terms.

11. Computation of C_{p_3}

As seen above, it will be necessary to obtain a C_{p_3} based on the velocity potential Φ_3 before the total C_p may be found. C_{p_3} may be found readily

from the derivative of Φ_3 with respect to x when evaluated at r = 1, which is

$$\left.\frac{\partial \Phi_3}{\partial \alpha}\right|_{r=1} = -\frac{V_\infty \alpha_B}{\pi}\left\{\frac{\sqrt{x^2 - 2(1 - \cos\theta)}}{x^2 - 1} + \frac{\sqrt{x^2 - 2(1 + \cos\theta)}}{x^2 - 1}\right.$$

$$+ \frac{\cos\theta}{(1 - x^2)^{3/2}}\cos^{-1}\frac{x^2 - (1 - \cos\theta)}{\sqrt{x^2 - \sin^2\theta}} - \frac{\cos\theta}{(1 - x^2)^{3/2}}\cos^{-1}$$

$$\left.\frac{x^2 - (1 + \cos\theta)}{\sqrt{x^2 - \sin^2\theta}} - \sin^{-1}\frac{\cos\theta - 1}{\sqrt{x^2 - \sin^2\theta}} + \sin^{-1}\frac{\cos\theta + 1}{\sqrt{x^2 - \sin^2\theta}}\right\}. \qquad (23)$$

The first and third terms contribute to $\partial\Phi_3/\partial x|_{r=1}$ only inside the Mach cone with apex at x = 0, y = +1, and x = 0, while the second and fourth terms contribute only inside the Mach cone with apex at x = 0, y = -1, and z = 0. The fifth and sixth terms give a variable contribution inside their respective Mach cones and a constant contribution outside their Mach cones. Once $\partial\Phi_3/\partial x|_{r=1}$ is known, it is a simple matter to obtain C_{p_3} as long as only first-order terms are retained in the expression for the pressure coefficient, since then

$$C_{p_3} = -2\frac{\left.\frac{\partial \Phi_3}{\partial x}\right|_{r=1}}{V_\infty} . \qquad (24)$$

12. Curves of C_p due to Interference of Wing on the Body

The various values of C_{p_3} and C_{p_4} have been combined according to Equation (22) and are plotted in Fig. 6. These curves have been nondimensionalized so that it is possible to find C_p on a cylindrical body at any angle of attack due to the presence of a flat-plate wing at zero angle of attack for any value of the free-stream Mach number for which the linearized approximations are valid. This nondimensionalization is accomplished by plotting $\beta C_p/\alpha_B$ versus x/β, where $\beta = \sqrt{M_\infty^2 - 1}$ for various values of θ.

The more practical problem of a flat-plate wing and a cylindrical body inclined at the same angle of attack with respect to the free stream may, of course, be solved by combining the solution presented here with the solution presented in Reference 2 as indicated at the beginning of this section. However, it is important to remember that this solution is applicable only forward of the Mach helix originating at the juncture of the body and the wing trailing edge.

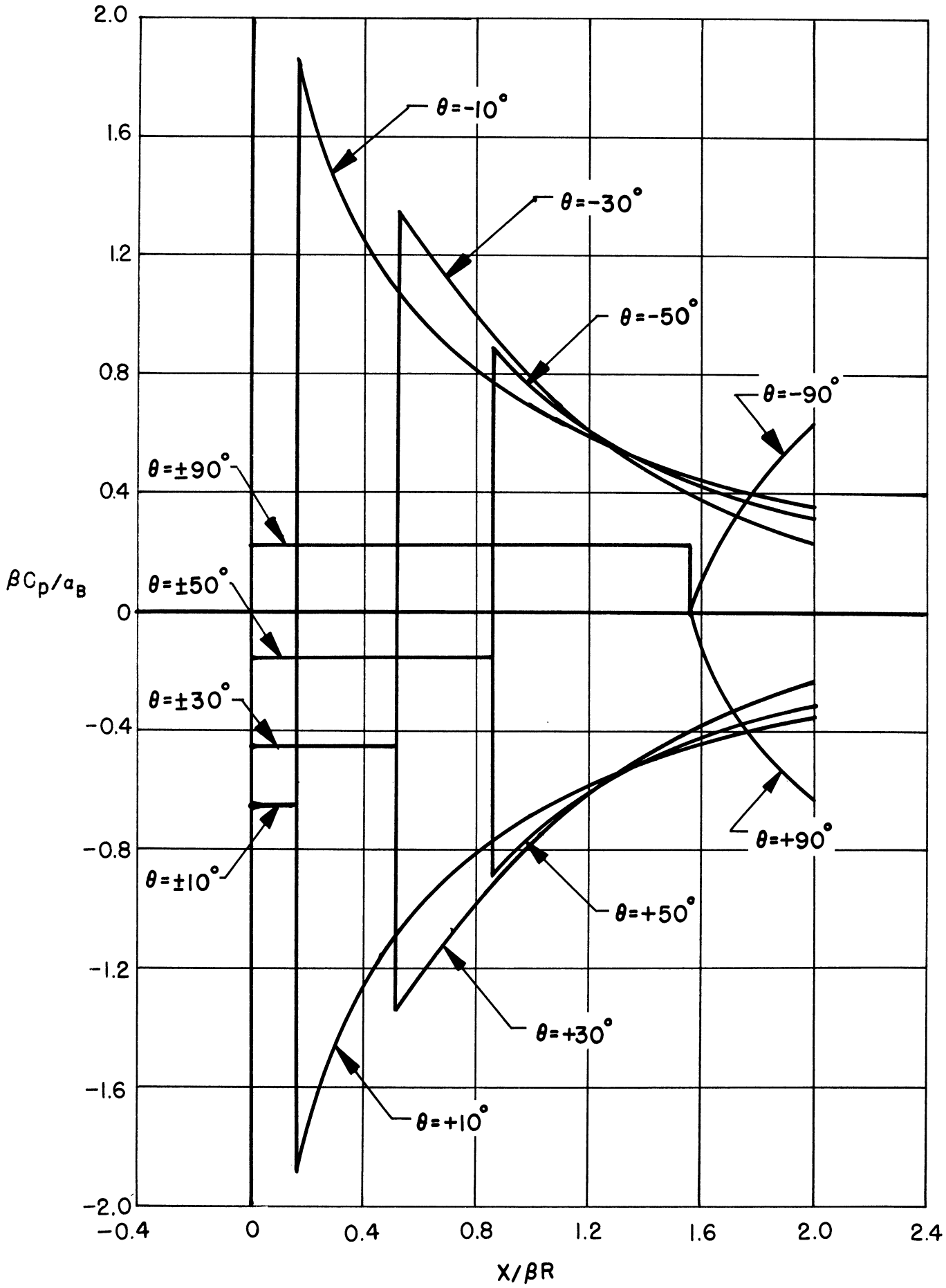

Fig. 6. Theoretical value of C_p on a cylindrical body at angle of attack α_B in the presence of a flat surface wing at zero angle of attack.

13. Corrections Applied to the Theoretical C_p Curves

As mentioned previously, the approximation of the pressure coefficient near a jump discontinuity by a Fourier series of only four terms will give a rather crude result. If the value of the jump and its position were known, it is probable that a considerably improved approximation to the actual value of the pressure coefficient curves could be obtained near the jump discontinuity.

As a consequence, the following procedure was used to obtain the value of the jumps in the pressure coefficient curves for the present problem. The axial position at which the jump discontinuity must occur is known to be on the Mach helix originating at the intersection of the wing leading edge and the cylindrical body. At intervals of $x = 0.2$ for x in the range $0 \leq x \leq 1.4$ the values of θ lying on this helix were computed. These values of θ were then substituted into the Fourier-series representation of C_p to obtain the value of C_p at the jump. Then, according to Reference 9, this value of C_p is approximately one-half of the actual jump in C_p. If, therefore, the values of $2C_p$, where C_p is the value obtained from the Fourier series, are plotted versus x, then the resulting curve should approximate the variation in the jump discontinuity along the Mach helix. Actually, in both cases this curve was found to be linear within the accuracy of the method. From this curve the value of the jump discontinuity for any desired meridional angle may be found if use is made of the equation defining the Mach helix, $\theta = x$.

Once the value of the curve at the jump is known as well as the four-term Fourier-series representation of the curve, a smooth curve may be faired through these data. This faired curve should give a fairly good approximation to the actual value of the pressure coefficient curve.

III. CONCLUSIONS

The solution presented here may be used in combination with the solution of References 2 and 3 to obtain the pressure distribution on a cylindrical body due to the presence of a flat surface wing for any combination of body and wing angles of attack. This solution, of course, is valid only forward of the trailing edge of the wing.

REFERENCES

1. Phinney, R. E., "Wing-Body Interference," Progress Report No. 4. Univ. of Mich. Eng. Res. Inst. Project M937, April, 1952.

2. Nielsen, J. N., "Supersonic Wing-Body Interference." Ph.D. Thesis, California Institute of Technology, 1951.

3. Nielsen, J. N., and Pitts, W. C., "Wing-Body Interference at Supersonic Speeds with an Application to Combinations with Rectangular Wings," NACAXTN2677, April, 1952.

4. Tsien, H. S., "Supersonic Flow over an Inclined Body of Revolution," Journal of the Aeronautical Sciences, 5, No. 12 (1938).

5. Dye, F. E., "A Comparison of Pressures Predicted by Exact and Approximate Theories with Some Experimental Results on an Ogival-Nosed Body at a Mach Number of 2.00," Cornell Report CAL/CF-1723, December, 1951.

6. Pierce, B. O., A Short Table of Integrals, Ginn and Company, 1929.

7. Milne-Thomson, L. M., Jacobian Elliptic Function Tables, Dover Publications, Inc., 1950.

8. Spenceley, G. W., and Spenceley, R. M., Smithsonian Elliptic Functions Tables, Smithsonian Institution, November 1, 1947.

9. Carslaw, H. S. Fourier Series and Integrals, Dover Publications, Inc., 1930.